© 2018. Published by The Company of Biologists Ltd | Development (2018) 145, dev156380. doi:10.1242/dev.156380

STEM CELLS AND REGENERATION

RESEARCH ARTICLE

ERECTA-family genes coordinate stem cell functions between the epidermal and internal layers of the shoot apical meristem

Yuka Kimura[1,2], Masao Tasaka[3], Keiko U. Torii[1,2,4,5,*] and Naoyuki Uchida[1,2,*]

ABSTRACT

The epidermal cell layer and the tissues that lie underneath have different intrinsic functions during plant development. The stem cells within the shoot apical meristem (SAM) that give rise to aerial structures are located in the epidermal and internal tissue layers. However, our understanding of how the functions of these stem cells are coordinated across tissue layers so stem cells can behave as a single population remains limited. WUSCHEL (WUS) functions as a master regulator of stem cell activity. Here, we show that loss of function in the ERECTA (ER)-family receptor kinase genes can rescue the mutant phenotype of *wus* plants (loss of stem cells), as demonstrated by the reinstated expression of a stem cell marker gene in the SAM epidermis. Localized *ER* expression in the epidermis can suppress the SAM phenotype caused by loss of ER-family activity. Furthermore, the CLAVATA3- and cytokinin-induced outputs, which contribute to stem cell homeostasis, are dysfunctional in a tissue layer-specific manner in ER-family mutants. Collectively, our findings suggest that the ER family plays a role in the coordination of stem cell behavior between different SAM tissue layers.

KEY WORDS: CLAVATA3, Cytokinin, ERECTA family, Shoot apical meristem, Stem cell, WUSCHEL

INTRODUCTION

Aerial plant tissues are derived from a population of stem cells in the shoot apical meristem (SAM), which is located at the shoot tip (Gordon et al., 2009; Miwa et al., 2009; Yadav et al., 2010). The SAM consists of three tissue layers: the epidermal L1 layer (tunica) and the internal layers L2 and L3 (corpus). Although these different tissue layers play distinct roles during development, stem cells are spread between them in the central zone of the SAM (Meyerowitz, 1997). We currently have a poor understanding of the molecular mechanisms that regulate how stem cells in the different SAM tissue layers are coordinated to behave as one population.

WUSCHEL (WUS) is a transcription factor that promotes stem cell proliferation, and *WUS* is expressed in the SAM-organizing center (OC). The *wus* mutants fail to maintain stem cells in the SAM (Laux et al., 1996; Mayer et al., 1998). *CLAVATA3* (*CLV3*) encodes a secreted peptide that suppresses *WUS* activity and is specifically expressed in the stem cells, thereby contributing to stem cell homeostasis (Brand et al., 2000; Schoof et al., 2000). Induction of the *WUS* expression is directly regulated by cytokinin signal transduction components, namely type-B ARABIDOPSIS RESPONSE REGULATOR proteins (ARRs) (Meng et al., 2017; Wang et al., 2017). Mathematical models have proposed that the cytokinin influences the *WUS* expression via cytokinin receptors expressed in the OC (Adibi et al., 2016; Chickarmane et al., 2012; Gordon et al., 2009; Gruel et al., 2016). Moreover, in turn, *WUS* promotes the cytokinin responsiveness of the SAM (Leibfried et al., 2005). However, the molecular mechanisms that underlie how the primary cytokinin response in the OC affects other SAM tissues remain unknown. In addition, in contrast to the well-characterized function of *WUS* in stem cell maintenance, we have a limited understanding of the role that *WUS*-independent mechanisms play in this process (Huang et al., 2015; Lee and Clark, 2015).

ERECTA (*ER*), *ER-LIKE1* (*ERL1*) and *ERL2* constitute the ER receptor kinase gene family (Shpak et al., 2004). All of these genes are expressed throughout the SAM and regulate its development (Bemis et al., 2013; Chen et al., 2013; Uchida et al., 2011, 2013). The *er erl1 erl2* triple mutant exhibits an expanded SAM with an enlarged stem cell region (Chen et al., 2013; Uchida et al., 2013). Furthermore, loss of function of ER-family members sensitizes SAM cell proliferation to cytokinin (Uchida et al., 2013). However, it remains largely unknown how *ER* activity affects the *CLV3-WUS* and cytokinin-signaling pathways, which contribute to stem cell maintenance.

Here, we report that loss of function of ER family restores the SAM in *wus* mutants, as demonstrated via the epidermis-specific expression of a stem cell marker gene. This phenotype caused by loss of ER-family activity is suppressed by localized *ER* expression in the epidermis. Furthermore, the CLV3 and cytokinin signaling pathways are dysfunctional in a tissue layer-specific manner in ER-family mutants. This study demonstrates that the ER family is required for the coordination of stem cell behavior between different SAM tissue layers.

RESULTS

SAM loss in *wus* plants is suppressed by attenuation of ER-family activity

A previous study reported that the vegetative SAM is enlarged in *er erl1 erl2* mutants compared to that in wild type (Uchida et al., 2013) (Fig. 1A,B,E,F; Fig. S1). Conversely, in *wus* mutants, the SAM is consumed soon after germination (Laux et al., 1996; Mayer et al., 1998; Fig. 1C,G; Fig. S1). To investigate the genetic interaction between ER family and *WUS*, and to address the relationship between their contrasting mutant phenotypes, we created a *wus er erl1 erl2* quadruple mutant. In *wus er erl1 erl2*, the SAM was maintained despite *WUS* loss of function (Fig. 1D,H; Fig. S1), and small cells characteristic of the wild-type SAM (Fig. 1E) were

[1]Institute of Transformative Bio-Molecules (WPI-ITbM), Nagoya University, Furo-cho, Chikusa-ku, Nagoya, 464-8601, Japan. [2]Division of Biological Science, Graduate School of Science, Nagoya University, Furo-cho, Chikusa-ku, Nagoya, 464-8602, Japan. [3]Graduate School of Biological Sciences, Nara Institute of Science and Technology, 8916-5 Takayama, Ikoma, 630-0192, Japan. [4]Department of Biology, University of Washington, Seattle, WA 98195, USA. [5]Howard Hughes Medical Institute, University of Washington, Seattle, WA 98195, USA.

*Authors for correspondence (ktorii@u.washington.edu, uchinao@itbm.nagoya-u.ac.jp)

K.U.T., 0000-0002-6168-427X; N.U., 0000-0002-4123-6154

Received 22 June 2017; Accepted 20 November 2017

Development (2018) 145, dev156380. doi:10.1242/dev.156380

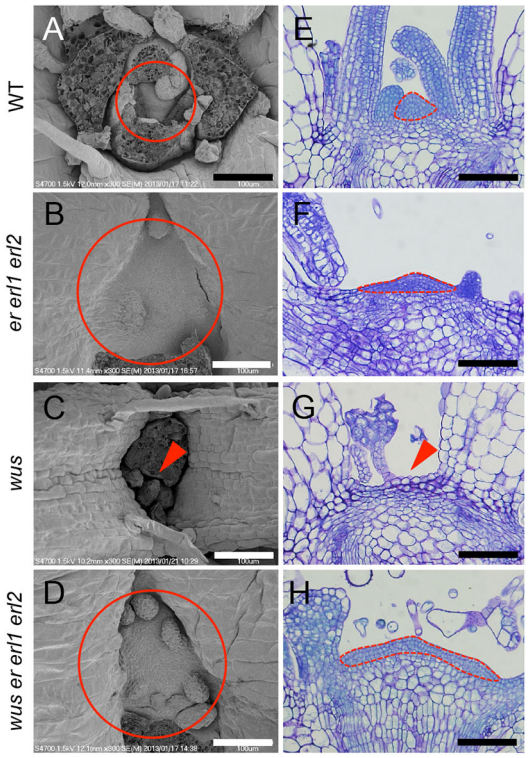

Fig. 1. SAM loss in the *wus* mutant is suppressed by ER-family loss of function. (A-D) Shoot apices of 10-day-old plants of various genotypes as observed by scanning electron microscopy. The images depicted are representative of those samples used for the quantitative analysis described in Fig. S1. Circles indicate SAM positioning. Arrowheads indicate a lack of SAM tissue. Scale bars: 100 µm. (E-H) Toluidine Blue-stained sections of SAM tissue of various genotypes. Dotted lines indicate the small-sized cell region that is characteristic of SAMs. Arrowhead indicates a lack of SAM tissue. Scale bars: 100 µm.

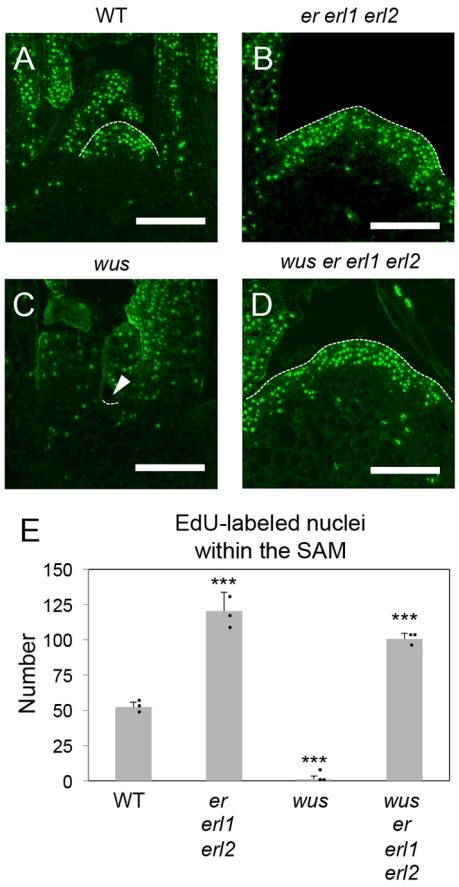

Fig. 2. Cell proliferation is maintained in the *wus er erl1 erl2* SAM. (A-D) Sections of 10-day-old plants of various genotypes with proliferating cells labeled by EdU. Dotted lines outline the SAM regions. The arrowhead in C indicates a lack of SAM tissue. Scale bars: 100 µm. (E) The number of EdU-labeled nuclei in the SAM region. Data are mean±s.d. ***P<0.005 compared with wild type, Student's t-test (two-tailed).

observed covering the surface of the *wus er erl1 erl2* SAM (Fig. 1H). Furthermore, the *wus er erl1 erl2* SAM persisted during the reproductive growth stage (Fig. S2). Although the SAM was consumed in *wus* (Fig. 1C,G), these *wus* plants occasionally produced adventitious meristems in later growth stages and formed adventitious inflorescences (Laux et al., 1996; Mayer et al., 1998). Accordingly, the emergence of the inflorescence stems in *wus* was severely delayed compared with that in wild type (Laux et al., 1996; Fig. S2A,B). By contrast, *wus er erl1 erl2* plants maintained the primary meristem (Fig. 1D,H), and bolted normally to form the primary inflorescence (Fig. S2A). Although the *wus* inflorescence developed few flowers (Fig. S2F,J), the *wus er erl1 erl2* inflorescence continuously produced flowers, comparable with that in wild type and *er erl1 erl2* mutants (Fig. S2C-E,G-I). Collectively, these observations suggest that ER-family loss of function largely alleviates the defects in both vegetative and inflorescence SAMs in *wus*. Furthermore, in contrast to the consistent lack of pistils in *wus* flowers (Laux et al., 1996), *wus er erl1 erl2* flowers formed pistils (Table S1). The number of stamens was also increased in *wus er erl1 erl2* compared with that in *wus*, whereas the numbers of sepals and petals were not recovered, suggesting that the complementation of *wus* flower formation imparted by ER-family lack of function was limited to the inner whorls.

To monitor cell proliferation in the SAM of *wus er erl1 erl2* mutants, we performed 5-ethynyl-2′-deoxyuridine (EdU) labeling. EdU incorporates into newly synthesized DNA to label actively dividing cells. In wild type and *er erl1 erl2*, EdU-labeled nuclei were detected across multiple SAM tissue layers (Fig. 2A,B). However, in *wus*, few EdU-labeled nuclei were detected at the center of the shoot apex where the SAM was consumed (Fig. 2C,E). This result is consistent with the observation that the small cells characteristic of SAMs in the wild-type and *er erl1 erl2* plants (Fig. 1E,F) were not apparent in *wus* (Fig. 1G). Interestingly, the *wus er erl1 erl2* SAM exhibited EdU-labeled nuclei similar to the *er erl1 erl2* SAM (Fig. 2B,D,E), demonstrating that cell proliferation is active in the *wus er erl1 erl2* SAM despite the loss of function of *WUS*. When the number of EdU-labeled nuclei was normalized to the SAM area, the normalized values were very similar among wild type, *er erl1 erl2* and *wus er erl1 erl2* (Fig. S3), indicating that cells in the SAM proliferate at a similar rate in these plants.

Stem cell markers are detected in the epidermal layer of the *wus er erl1 erl2* SAM

CLV3pro:GUS is a known and reliable stem cell marker; however, GUS signal is not observed in the SAM of *wus* plants (Brand et al., 2002; Fig. 3A,B). Conversely, *CLV3pro:GUS* expression produced a detectable GUS signal at the periphery (Fig. 3C, arrow) and in the central region of the SAM in *er erl1 erl2*, which likely reflects SAM expansion in the absence of ER-family activity. Furthermore, a

Development (2018) 145, dev156380. doi:10.1242/dev.156380

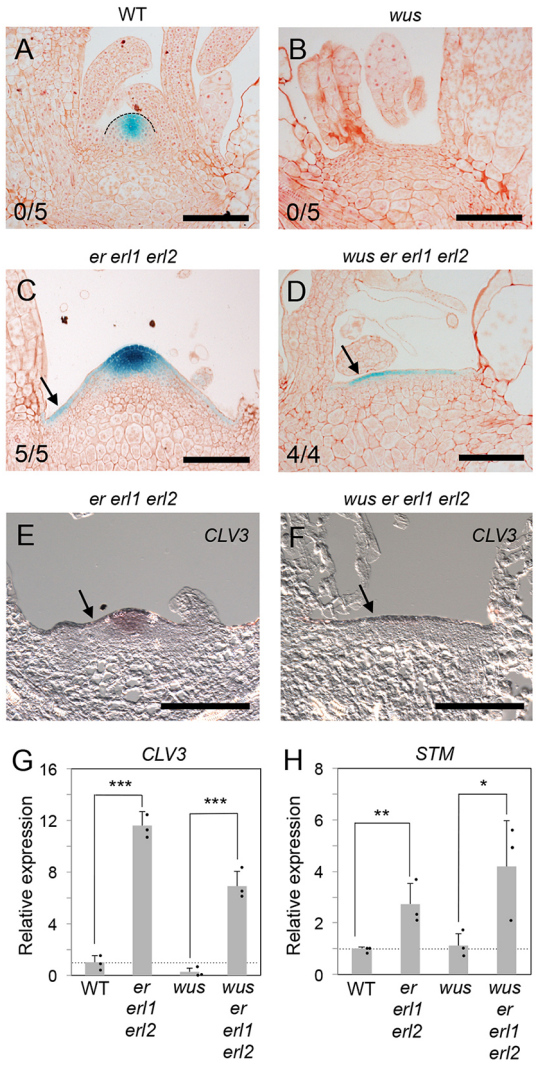

Fig. 3. *CLV3pro:GUS* expression is specifically maintained in the epidermis of the *wus er erl1 erl2* SAM. (A-D) *CLV3pro:GUS* signals in sections of SAM tissue from 10-day-old plants of various genotypes. Scale bars: 100 µm. Arrows indicate *CLV3pro:GUS* signal localized to the epidermis. The proportion of examined plants displaying an epidermis-specific GUS signal is indicated in the lower left corner of each panel. (E,F) *In situ* RNA hybridization experiments to detect endogenous *CLV3* expression patterns. Scale bars: 100 µm. Arrows indicate signals localized to the epidermis. (G,H) *CLV3* (G) and *STM* (H) transcript levels in shoot apices normalized against *β-TUBULIN* expression. Expression levels in mutant lines are related to that in the wild type, which was set to 1. Ten individual plants were pooled for each sample. The mean of three biological replicates±s.d. is shown. **P*<0.05, ***P*<0.01 and ****P*<0.005, Student's *t*-test (two-tailed). The compensatory expression of *STM* was detected in *wus*, as reported previously (Mayer et al., 1998).

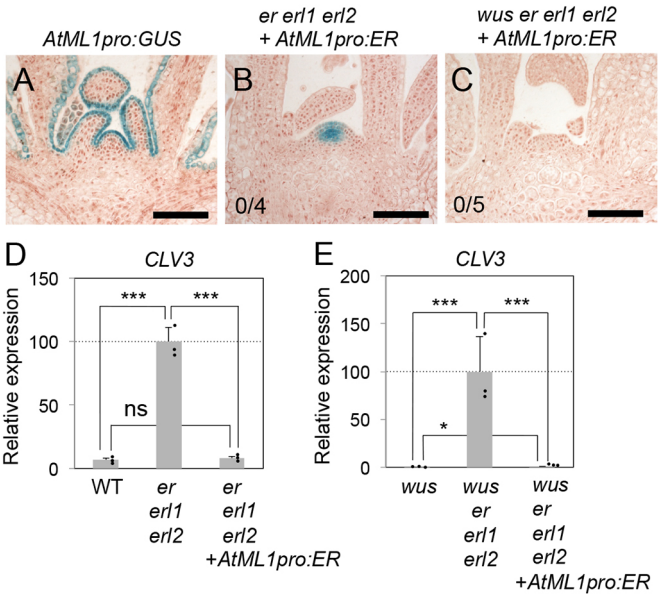

Fig. 4. *ER* expression in the epidermis rescues the altered *CLV3pro:GUS* expression in *er erl1 erl2* mutants. (A) *AtML1pro:GUS* signal in a SAM section of a 10-day-old wild-type plant. Scale bar: 100 µm. (B,C) *CLV3pro:GUS* signal in SAM sections of 10-day-old plants of mutant lines complemented with *AtML1pro:ER*. Depicted images are representative of four to five independent samples analyzed for each genotype. Scale bars: 100 µm. The proportion of examined plants that displayed an epidermis-specific GUS signal is indicated in the lower left corner of each panel. (D,E) *CLV3* transcript levels in shoot apices normalized against *β-TUBULIN* expression. Expression levels among plant genotypes are related to those in *er erl1 erl2* (D) and *wus er erl1 erl2* (E), which were set to 100. Five to six individual plants were pooled for each sample. The mean of three biological replicates±s.d. is shown. ****P*<0.005 and **P*<0.05, Student's *t*-test (two-tailed). ns, not significant.

strong GUS signal was detected in the SAM epidermal layer in *wus er erl1 erl2* plants (Fig. 3D). *In situ* RNA hybridization experiments also showed the epidermal expression of endogenous *CLV3* in the mutants (Fig. 3E,F), indicating the consistency between the extended epidermal *CLV3pro:GUS* signal and the *CLV3* transcript accumulation. These results demonstrate that ER-family loss of function allows expression of the stem cell marker in the SAM epidermis even in the absence of WUS activity (Fig. 3D); however, WUS is required for *CLV3pro:GUS* expression in the full complement of SAM tissue layers, as is observed in the wild type (Fig. 3A) and not in *wus er erl1 erl2* (Fig. 3D). Thus, in the absence of ER-family activity, the dependence of stem cell marker expression on *WUS* is decoupled between the epidermis and the internal tissue. Recovery of stem cells in *wus er erl1 erl2* was also confirmed using qRT-PCR analysis, which revealed strong expression of endogenous *CLV3* in the quadruple mutant (Fig. 3G). *SHOOT MERISTEMLESS* (*STM*) expression levels (Long et al., 1996) were also examined as a marker gene indicative of undifferentiated cells. We observed high-level *STM* expression in *wus er erl1 erl2* plants (Fig. 3H), which is consistent with the enlarged SAM observed in these plants (Fig. 1D,H).

ER expression in the SAM epidermis complements the *CLV3pro:GUS* expression phenotype of the *er erl1 erl2* mutants

Expression of *CLV3pro:GUS* produced a GUS signal in the epidermal cells at the periphery of the SAM in *er erl1 erl2* mutants (Fig. 3C, arrow), and the *CLV3pro:GUS* expression in the epidermis was still maintained in *wus er erl1 erl2* (Fig. 3D). These results suggest that, although *ER* is expressed throughout the SAM (Uchida et al., 2013; Fig. S4A), the *ER* activity in the epidermis may directly function to regulate the stem-cell-marker signals in the epidermal cells. To investigate this potential role further, we performed complementation experiments by expressing *ER* in *er erl1 erl2* and *wus er erl1 erl2* under the control of the epidermis-specific *AtML1* promoter (Sessions et al., 1999; Fig. 4A). Compared with the broad *CLV3pro:GUS* expression pattern observed in *er erl1 erl2* (Fig. 3C), we observed no GUS signal in the epidermal cells at the periphery of the SAM in *er erl1 erl2 AtML1pro:ER* plants

Development (2018) 145, dev156380. doi:10.1242/dev.156380

(Fig. 4B), and *CLV3pro:GUS* expression in these complemented plants was restricted to a compact region at the center of the normally sized SAM (Fig. 4B) as seen in the wild-type plants (Fig. 3A). On the other hand, the expression of *ER* in *er erl1 erl2* under the control of the OC-specific *WUS* promoter did not rescue either the *CLV3pro:GUS* misexpression at the SAM periphery or the enlarged SAM morphology (Fig. S4F), emphasizing the importance of the *ER* function in the epidermis to prevent the misexpression of the stem cell marker. Accordingly, the elevated expression of endogenous *CLV3* observed in *er erl1 erl2* was decreased in *er erl1 erl2 AtML1pro:ER* to a level comparable with that in wild type (Fig. 4D). In addition, *AtML1pro:ER* largely ameliorated dwarfism and small leaf phenotype of *er erl1 erl2* seedlings (Fig. S4C,D), whereas *WUSpro:ER* did not affect the seedling phenotypes (Fig. S4E). However, the petiole length of *er erl1 erl2 AtML1pro:ER* leaves appeared intermediate between those of wild type and *er erl1 erl2* (Fig. S4B-D), suggesting that ER functions in non-epidermal tissues may also contribute to the petiole growth.

We observed similar results for *wus er erl1 erl2 AtML1pro:ER*. Following *AtML1pro:ER* expression, the epidermal *CLV3pro:GUS* expression observed in *wus er erl1 erl2* was no longer apparent (Figs 3D and 4C) and the high endogenous *CLV3* expression observed in *wus er erl1 erl2* was also considerably reduced (Fig. 4E). These results indicate that *ER* activity in the epidermis contributes to the maintenance of SAM homeostasis. Furthermore, *AtML1pro:ER* expression improved the small leaf phenotype of *wus er erl1 erl2* (Fig. S4H,I), suggesting that the *ER* activity in the epidermis promotes leaf growth.

A loss of ER-family activity disrupts the CLV3 signaling outputs in a tissue layer-specific manner

The CLV3 peptide, which is secreted from stem cells, plays an important role in regulating SAM homeostasis and treatment with exogenous CLV3 peptide can lead to the loss of both SAM structure and the SAM stem cell population (Kondo et al., 2006; Fig. 5A,B,E,F,M,N,Q,R, Fig. S5). Therefore, we addressed whether the ER family regulates CLV3 signaling by treating ER-family mutants with CLV3. The SAM was maintained in *er erl1 erl2* in the presence of excess CLV3 peptide (Fig. 5C,D,G,H; Fig. S5), indicating that mutation of the ER family interferes with CLV3 signaling. In agreement, GUS signals arising from expression of *CLV3pro:GUS* as well as *WUSpro:GUS*, a marker of the OC (Laux et al., 1996; Mayer et al., 1998), were maintained in the *er erl1 erl2* SAM following CLV3 treatment (Fig. 5K,L,O,P). By contrast, in the wild type, CLV3 application abolished the expression of both *CLV3pro:GUS* and *WUSpro:GUS* (Fig. 5I,J,M,N,Q,R).

Closer inspection of the *CLV3pro:GUS* expression pattern in *er erl1 erl2* revealed that the effects of CLV3 treatment differed between the epidermal and the internal tissue layers (Fig. 5S-V; Fig. S6). CLV3 peptide did not affect *CLV3pro:GUS* expression in the epidermis (Fig. 5S-U), as the extent of epidermal GUS signal was not reduced upon CLV3 treatment in the *er erl1 erl2* mutant (Fig. 5U). However, GUS signal in the internal tissue layers was significantly diminished (Fig. 5S,T,V). Thus, *er erl1 erl2* stem cells situated in the internal tissue layers, but not the epidermal stem cells, retained the ability to respond to CLV3 signaling. These findings were consistent with the decreased expression level of endogenous *CLV3* in *er erl1 erl2* following CLV3 peptide treatment (Fig. 5W). Moreover, the SAM in *clv3 er erl1 erl2* was larger than that in *clv3* and *er erl1 erl2* (Fig. 6; Fig. S7), suggesting that SAM development remains responsive to CLV3 signaling in *er erl1 erl2,* most likely via the influence of CLV3 on the internal tissue layers of the SAM. By contrast, *CLV3pro:GUS* expression in both the SAM epidermal and internal tissue layers in the wild type was similarly influenced by CLV3 peptide treatment (Fig. 5Q,R,U,V). Collectively, these results indicate that ER-family activity is required for the coordination of CLV3 signaling responses between the SAM epidermal and internal tissue layers.

In addition to its effect on the SAM, CLV3 treatment also affects root growth (Fiers et al., 2005; Kondo et al., 2006). In contrast to CLV3 responses in the SAM described above, the CLV3 peptide inhibited root growth in both wild type and *er erl1 erl2* (Fig. S8), indicating that the ER-family mutation does not affect CLV3 signaling in roots.

The loss of ER-family activity decouples the regulation of SAM homeostasis by cytokinin signaling between the SAM epidermal and internal tissue layers

Cytokinin acts as an important regulator of SAM homeostasis (Chickarmane et al., 2012; Gordon et al., 2009), and WUS promotes the responsiveness of the SAM to cytokinin (Leibfried et al., 2005). Based on the variation between the SAM epidermal and internal tissue layers in the absence of *WUS* activity in *er erl1 erl2* mutants (Fig. 3), we hypothesized that the cytokinin signaling-mediated regulation of SAM homeostasis might also be modulated by the ER family in a tissue layer-specific manner. To investigate this, we analyzed cytokinin responses using the synthetic cytokinin response marker *TCSn:GFP* (Zurcher et al., 2013). Using this reporter, we detected the GFP signal in the OC of the wild-type SAM (Fig. 7A), consistent with previous reports (Chickarmane et al., 2012), and this GFP signal was maintained in the *er erl1 erl2* mutant SAM (Fig. 7B). These *TCSn:GFP* expression patterns are consistent with the similar expression levels of cytokinin receptor and *type-B ARR* genes, which are positive regulators of cytokinin signaling (Meng et al., 2017; Wang et al., 2017), between *er erl1 erl2* and wild type (Fig. S9). These results suggest that the primary cytokinin response is not disturbed in *er erl1 erl2*.

To examine the effects of ER-family activity on the stem cell behaviors under perturbed cytokinin signaling, we employed the *wooden leg* (*wol*) allele, a dominant-negative mutation in the OC-expressed cytokinin receptor gene *ARABIDOPSIS HISTIDINE KINASE 4* (*AHK4*) that inhibits cytokinin receptor signaling (Mähönen et al., 2000). We observed a reduction in both SAM size and the extent of *CLV3pro:GUS* expression in the *wol* mutant (Fig. 7C,E), which agrees with the known phenotypes of cytokinin-deficient mutants (Werner et al., 2003). Moreover, *CLV3pro:GUS* expression was similarly reduced in both the SAM epidermal and internal tissue layers in *wol* (Fig. 7I,K), whereas in the *er erl1 erl2 wol* SAM, *CLV3pro:GUS* expression was reduced only in the internal tissue layers (Fig. 7D,F,J,L). Furthermore, a pharmacological approach based on treatment with the cytokinin receptor antagonist S-4893 (Arata et al., 2010) revealed expression patterns that corroborated those observed in *wol* (Fig. 7G-L). Therefore, in the ER-family mutant SAM epidermis, the expression of this stem cell marker is resistant to the loss of cytokinin signaling, whereas the maintenance of this marker expression in the SAM internal tissue layers requires cytokinin signaling.

Taken together, our data indicate that, in the maintenance of proper SAM homeostasis, the ER-family genes are required for the coordination of stem cell behaviors between the epidermal and internal tissue layers. Without ER-family activity, the influence of *WUS*, *CLV3* and cytokinin on stem cells is decoupled between the different SAM tissue layers.

Development (2018) 145, dev156380. doi:10.1242/dev.156380

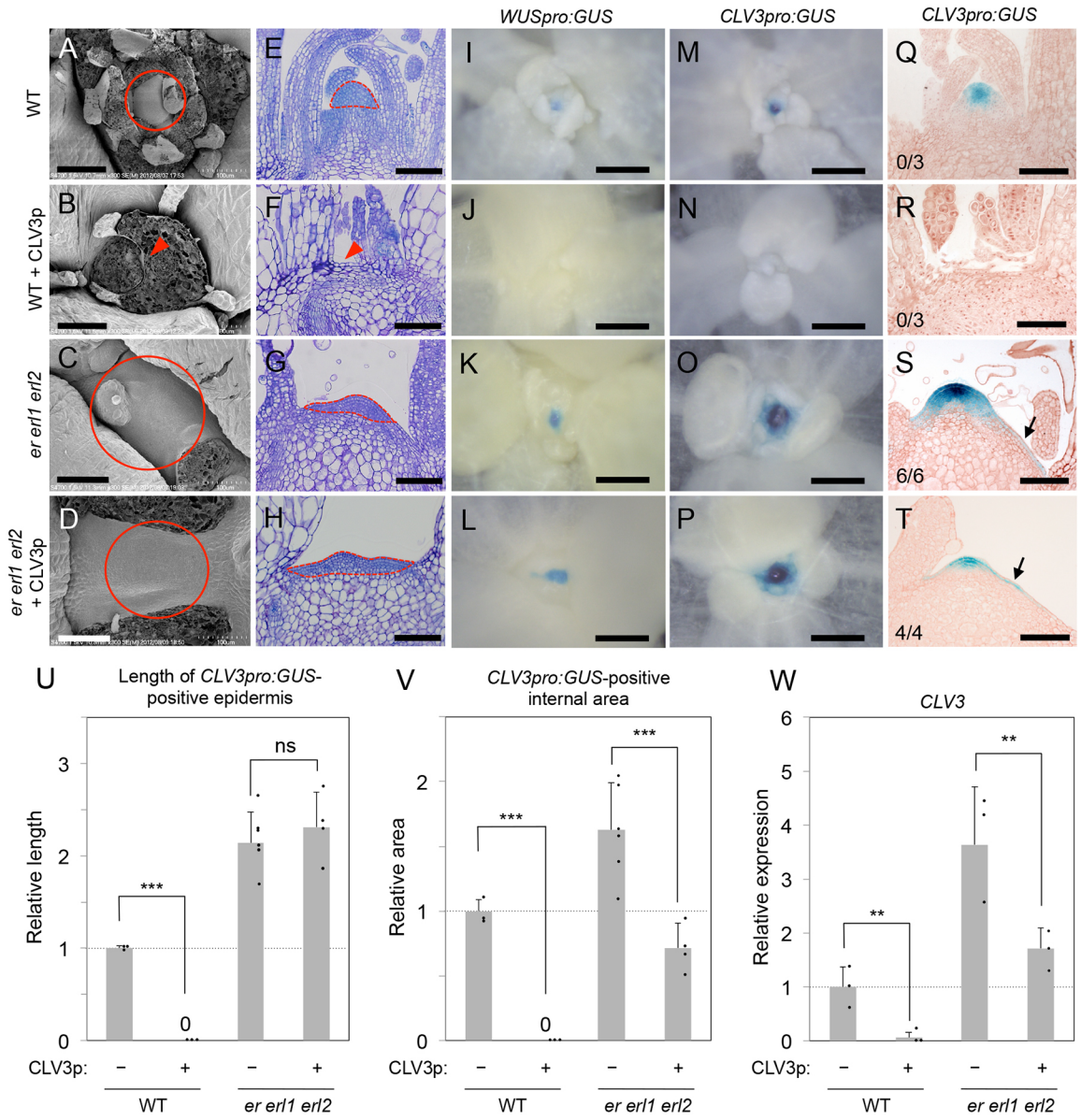

Fig. 5. The effect of CLV3 peptide treatment on *CLV3pro:GUS* expression varies in *er erl1 erl2* in a tissue layer-specific manner. Analyses of 12-day-old plants following treatment with 5 µM CLV3 peptide (CLV3p). (A-D) Shoot apices observed by scanning electron microscopy. The depicted images are representative of those samples used for the quantitative analysis described in Fig. S5. Circles indicate SAM positioning. Arrowhead indicates a lack of SAM tissue. Scale bars: 100 µm. (E-H) Toluidine Blue-stained sections of SAM tissues of various genotypes. Dotted lines indicate the small cell region that is characteristic of SAMs. Arrowhead indicates a lack of SAM tissue. Scale bars: 100 µm. The depicted images are representative of three independent samples analyzed for each genotype and treatment. (I-P) GUS signal resulting from *WUSpro:GUS* (I-L) and *CLV3proGUS* (M-P) expression in various genotypes. The depicted images are representative of three independent samples analyzed for each genotype and treatment. Scale bars: 200 µm. (Q-T) GUS signal resulting from *CLV3pro:GUS* expression in SAM sections of various genotypes. The depicted images are representative of three to six independent samples analyzed for each genotype and treatment. Scale bars: 100 µm. The proportion of examined plants displaying an epidermis-specific GUS signal at the periphery of the SAM is indicated in the lower left corner of each panel. (U,V) Quantitation of epidermis length (U) and internal SAM area (V) exhibiting GUS signal from *CLV3pro:GUS* expression. The method to measure length and area is explained in Fig. S6. The mean±s.d. is shown. ***P<0.005, Student's *t*-test (two-tailed). ns, not significant. (W) *CLV3* expression in shoot apices as normalized against *β-TUBULIN* expression. Expression levels are related to that in the wild type, which was set to 1. Twenty individual plants were pooled for each sample. The mean of three biological replicates±s.d. is shown. **P<0.01, Student's *t*-test (two-tailed).

DISCUSSION

ER-family activity suppresses *WUS*-independent processes for the maintenance of SAM homeostasis

We demonstrated that the SAM stem cell loss observed in *wus* mutants is suppressed by loss of function of ER-family members (Fig. 1). Recent studies also reported that the mutations *altered meristem program 1* (*amp1*) and *class III homeodomain-leucine zipper* (*hd-zip III*) partially complement the *wus* phenotype by promoting the production of adventitious SAMs (Huang et al., 2015; Lee and Clark, 2015). However, there are clear differences between the effects of *er erl1 erl2*, *amp1* and *hd-zip III* on the *wus* phenotype. Although *amp1* and *hd-zip III* contribute to the formation of adventitious SAMs in *wus*, the primary SAM is still consumed in these mutants. By contrast, the primary SAM is recovered in *wus er erl1 erl2* (Fig. 1). Furthermore, *wus er erl1 erl2* produces flowers with pistils (Table S1), whereas *wus hd-zip III*

Development (2018) 145, dev156380. doi:10.1242/dev.156380

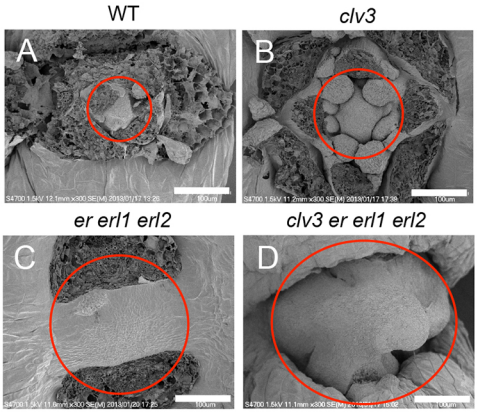

Fig. 6. The regulation of SAM size by *CLV3* is functional in *er erl1 erl2* mutants. (A-D) Shoot apices of 10-day-old plants as observed by scanning electron microscopy. The depicted images are representative of those samples used for the quantitative analysis presented in Fig. S7. Circles indicate SAM tissue regions. Scale bars: 100 µm.

develops *wus*-like flowers that lack pistils (Lee and Clark, 2015). Thus, the ER family seems to function in a different manner from *AMP1* and *HD-ZIP III*. This hypothesis agrees with the finding that *jabba-1D,* which suppresses *HD-ZIP III*, results in an enlarged SAM in *er* mutants, suggesting that *HD-ZIP III* and *ER* act in parallel (Mandel et al., 2016, 2014). As *wus er erl1 erl2* maintains *CLV3pro:GUS* expression specifically in the SAM epidermis (Fig. 3D), which contrasts with the lack of GUS signal in all SAM tissue layers in *wus* (Fig. 3B), we proposed that *ER* suppresses *WUS*-independent processes that can maintain stem cells in the epidermis. We subsequently showed that localized *ER* expression in the epidermis is sufficient to suppress *WUS*-independent stem cell development (Fig. 4). Similarly, future research should focus on elucidating the SAM domains where *AMP1* and *HD-ZIPIII* act to regulate SAM homeostasis.

The relationship between *CLV3pro:GUS* expression and cell proliferation in the *wus er erl1 erl2* SAM

In wild-type plants, *CLV3pro:GUS* expression was detected in the epidermal L1 layer and the internal L2 and L3 layers in the SAM center (Fig. 3A), indicating that stem cells are located within each of these layers. The stem cells in the epidermal L1 layer and the subepidermal L2 layer divide anticlinally, whereas those in the L3 layer divide both anticlinally and periclinally (Meyerowitz, 1997). All of these stem cells supply daughter cells to surrounding tissues for organ formation. In contrast to the multiple tissue-layer expression observed in the wild type, *CLV3pro:GUS* expression was restricted to the epidermis in the *wus er erl1 erl2* SAM (Fig. 3D); however, cell proliferation was still detected in all SAM tissue layers (Fig. 2D). Moreover, our histological analyses revealed a population of small cells covering the *wus er erl1 erl2* SAM (Fig. 1H).

The inconsistency between *CLV3pro:GUS* expression and cell proliferation within the *wus er erl1 erl2* SAM can be explained in multiple ways. Periclinal division of stem cells in the *wus er erl1 erl2* SAM epidermis may supply daughter cells in the subepidermal tissue layers that may then proliferate, thereby maintaining the internal tissues. Alternatively, in addition to the observed canonical epidermal stem cells, there may be stem cells that do not express the *CLV3pro:GUS* marker in the internal tissue of the *wus er erl1 erl2* SAM. However, there is currently no evidence for the existence of *CLV3*-negative stem cells in the wild-type SAM, and future research

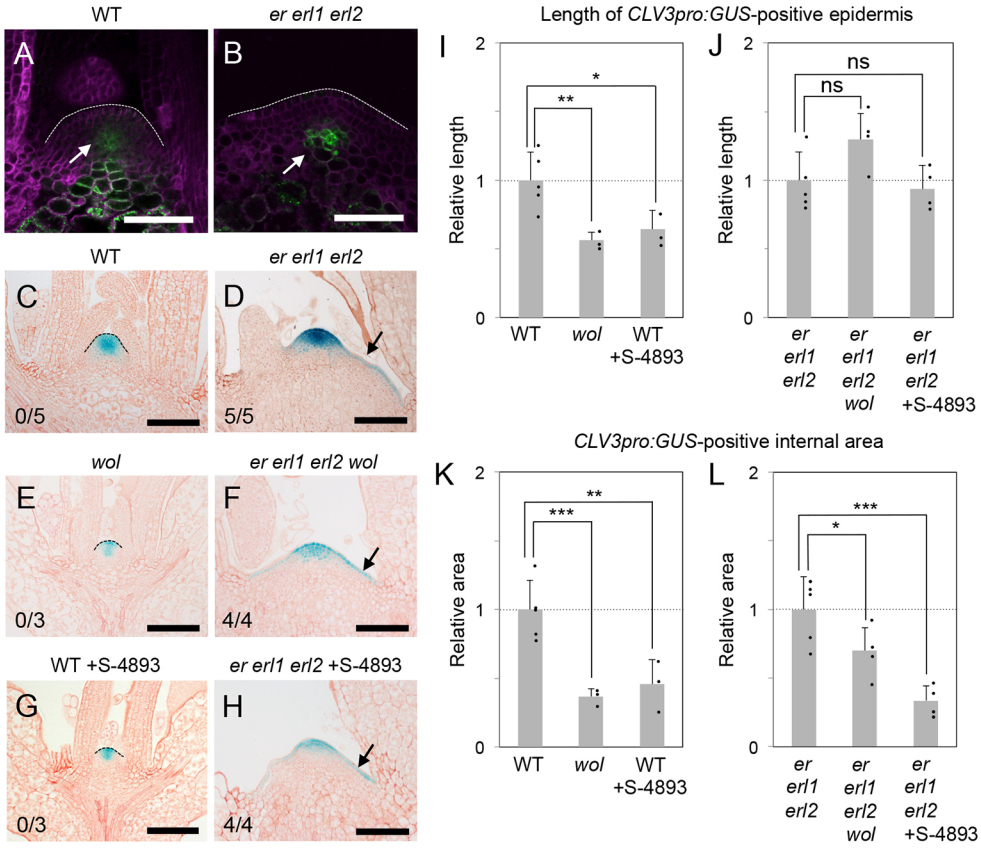

Fig. 7. Attenuated cytokinin signaling affects *CLV3pro:GUS* expression in a tissue layer-specific manner in *er erl1 erl2*. (A,B) *TCSn:GFP* signals (white arrows) in SAMs of 10-day-old seedlings. Magenta coloring indicates plasma membranes stained with FM4-64. Scale bars: 100 µm. (C-H) *CLV3pro:GUS* expression in SAM tissue sections from 10-day-old plants. Depicted images are representative of three to five independent samples analyzed for each genotype and treatment. Dotted lines indicate SAM tissue regions. Black arrows indicate *CLV3pro:GUS* signal localized to the epidermis. Scale bars: 100 µm. The proportion of examined plants displaying an epidermis-specific GUS signal is indicated in the lower left corner of each panel. (I-L) Length of SAM epidermis (I,J) and area of SAM tissue (K,L) exhibiting GUS signal from *CLV3pro:GUS* expression in wild-type (WT; I,K) and *er erl1 erl2* (J,L) backgrounds. The method behind length and area measurements is explained in Fig. S6. Data are mean±s.d. **P*<0.05, ***P*<0.01 and ****P*<0.005, Student's *t*-test (two-tailed). ns, not significant.

Development (2018) 145, dev156380. doi:10.1242/dev.156380

to examine this possibility would require the development of alternate reliable stem cell markers. For this purpose, the reported *Arabidopsis* SAM transcriptome (Yadav et al., 2009, 2014) may be used alongside the materials made in this study.

The ER family modulates non-cell-autonomous effects downstream of the primary cytokinin response in the SAM OC in a tissue layer-specific manner

Although the cytokinin response is primarily activated in the SAM OC alone (Adibi et al., 2016; Chickarmane et al., 2012; Gordon et al., 2009; Gruel et al., 2016), attenuation of cytokinin signaling results in an overall reduction in SAM size (Leibfried et al., 2005; Werner et al., 2003; Fig. 7C,E,G). This implies that a secondary signal exists that is activated following the primary cytokinin response in the OC, which would then non-cell-autonomously affect surrounding SAM cells. We showed that a normal cytokinin response was maintained in the OC of the *er erl1 erl2* SAM (Fig. 7B). However, in contrast to that seen in the wild-type SAM, *CLV3pro:GUS* expression in the *er erl1 erl2* SAM epidermis was not attenuated by cytokinin signaling (Fig. 7C-L). Thus, ER-family loss of function likely renders the epidermal stem cells independent of the non-cell-autonomous secondary signal that acts downstream of the primary cytokinin response in the OC. This hypothesis is consistent with the observed suppression of the *er erl1 erl2* phenotype by *ER* expression in the SAM epidermis (Fig. 4). It will be interesting to characterize the molecular nature of this secondary signal in future studies. Given that *WUS* is known to both modulate the cytokinin responsiveness of the SAM (Leibfried et al., 2005) and regulate the expression of hundreds of genes (Busch et al., 2010), the WUS transcription factor may regulate gene expression that leads to production of a secondary signal in the SAM OC. Furthermore, given the similar phenotypes resulting from both CLV3 peptide treatment (Fig. 5Q-V) and the attenuation of cytokinin signaling (Fig. 7C-L), CLV3 signaling may also regulate production of such a secondary signal.

Ligands for ER-family receptor proteins in stem cell regulation

ER-family loss of function renders the SAM insensitive to CLV3 peptide treatment in a tissue layer-specific manner (Fig. 5). However, it is unlikely that ER-family proteins directly perceive the CLV3 signal, as direct binding of the CLV3 peptide to its corresponding receptor CLV1 has been unambiguously demonstrated (Ogawa et al., 2008). Several EPIDERMAL PATTERNING FACTOR-LIKE (EPFL) secreted peptides have been identified as ligands for ER-family proteins in stomatal patterning, inflorescence morphogenesis and leaf serration (Abrash et al., 2011; Lee et al., 2015, 2012; Tameshige et al., 2016; Uchida et al., 2012). Therefore, EPFL-family members may act as a yet-uncharacterized signal upstream of the ER family in stem cell maintenance. Accordingly, we found that *EPFL1* and *EPFL2* are expressed in the shoot apex (Fig. S10), although it remains unclear whether these genes act in regulating SAM functions. In this study, we show that the localized *ER* expression in the epidermis is sufficient to rescue the misexpression of stem cell marker *CLV3* in the epidermis of ER-family mutants, whereas *ER* is expressed throughout the shoot apices (Uchida et al., 2013; Fig. S4A). Given that the shoot apex is a complex tissue composed of multiple domains, such as OC, the boundary region, the rib zone and the initiating primordia of lateral organs, it will be important in future research to delineate the individual functions of ER-family proteins in each domain and to elucidate whether the SAM-expressed EPFLs act through ER proteins in epidermal and/or non-epidermal domains.

Taken together, our findings indicate that ER-family receptor kinase genes coordinate stem cell behaviors between the SAM epidermal and internal tissue layers to ensure that all SAM stem cells behave as a single entity. Continuing research should focus on downstream events that regulate SAM stem cells following activation of ER-family signaling.

MATERIALS AND METHODS

Plant materials and growth conditions

The mutant lines *er erl1 erl2* (Shpak et al., 2004), *wus* (SAIL_150_G06) (Chatfield et al., 2013; Sonoda et al., 2007), *wol* (CS9817) (Mähönen et al., 2000), *CLV3pro:GUS* (Brand et al., 2002), *TCSn:GFP* (Zurcher et al., 2013), *AtML1pro:GUS* (Uchida et al., 2012), *AtML1pro:ER* (Uchida et al., 2012), *EPFL2pro:GUS* (Tameshige et al., 2016), *WUSpro:GUS* (Hirakawa et al., 2017) and *ERpro:ER-YFP* (Horst et al., 2015; Ikematsu et al., 2017) in Col have been reported previously. The mutant line *clv3-2* in L*er* was introgressed into Col three times and then crossed with *er erl1 erl2*. To engineer *clv3* with functional *ER*, the *ER* genomic fragment derived from Col (Godiard et al., 2003) was introduced into *clv3-2*. The primers used for amplification of the *WUS* and *EPFL1* promoter regions are listed in Table S2. *WUSpro:ER* was constructed according to the previously reported procedure for the *AtML1pro:ER* construction (Uchida et al., 2012). Plants were grown on Murashige and Skoog (MS) media at 22°C under continuous light. For chemical treatment, plants were grown on media containing either 5 µM 6-benzylaminopurine (BAP; Sigma, B3408), 5 µM CLV3 peptides (Operon) or 10 µM S-4893 (InterBioScreen, 1S-73130).

Scanning electron microscopy

Seedling tissue was fixed with 4% FAA and then dehydrated via an ethanol series using 50-100% ethanol solutions before the ethanol was gradually exchanged with 100% acetone followed by critical point drying. Leaves were removed from the dried samples and vapor deposition was performed by ion spatter (E-1010, Hitachi). Samples were then observed using a field emission scanning electron microscope (S-4700, Hitachi).

GUS staining and histology

Seedlings were treated with 90% acetone and incubated in a GUS staining solution [50 mM sodium phosphate buffer (pH 7.0), 10 mM potassium ferricyanide, 10 mM potassium ferrocyanide, 2 mM X-Gluc, 0.2% Triton-X] at 37°C. Samples were fixed with 4% FAA, embedded in Technovit7100 (Heraeus Kulzer) and sectioned using a microtome (Leica, RM2235). Sections were stained with either 0.04% Neutral Red or 0.02% Toluidine Blue. Quantitative analysis of the GUS signal in section images was performed using the ImageJ software. Cells exhibiting GUS signal in the internal tissue layers were selected using the polygonal lasso tool as shown in Fig. S6, and the selected area was quantified. GUS-stained epidermal cells were traced using the segmented line tool as shown in Fig. S6, and the length of the SAM epidermis exhibiting GUS signal was measured. *In situ* RNA hybridization experiments to detect *CLV3* transcripts were performed according to the previous report (Uchida et al., 2013).

Quantitative real-time PCR

Total RNA was extracted from 10-day-old shoot apices using an RNeasy Plant Mini Kit (Qiagen). qRT-PCR was performed using a ReverTra Ace qPCR RT Master Mix with gDNA Remover kit (TOYOBO), a SYBR Fast qPCR kit (KAPA) and a Light Cycler 96 (Roche). The primers used for expression analyses are listed in Table S2.

Confocal microscopy

Plant samples were embedded in 6% UltraPure Low Melting Point Agarose (Thermo Fisher), and then 70 µm sections were made using a vibrating microtome (Leica, VT1200S). Sections were mounted in water and stained with or without 25 µg/ml FM4-64 for counterstaining. GFP, YFP and FM4-64 fluorescence was observed by confocal microscopy (Leica, SP8 and

Development (2018) 145, dev156380. doi:10.1242/dev.156380

Zeiss, LSM800) with excitation at 488 nm. Emission ranges were 495-555 nm for GFP, 500-546 nm for YFP and 580-626 nm for FM4-64.

EdU labeling assay

Ten-day-old seedlings grown on solid MS media were incubated in ½ MS liquid medium containing 10 µM EdU (Click-iT EdU Alexa Fluor 488 imaging kit; Invitrogen) for 16 h. The seedlings were then treated with 90% acetone, washed three times with PBS, fixed with 4% FAA, embedded in Technovit7100 (Heraeus Kulzer), and sectioned using a microtome (LEICA, RM2235). The sections were treated with an Alexa Fluor 488 probe according to the manufacturer's protocol, and then fluorescence signals were observed by fluorescence microscopy (Zeiss, Axioimager A2 with FS 38HE filter).

Acknowledgements

We thank Dr Rüdiger Simon, Dr Bruno Müller and Dr Tatsuo Kakimoto for providing materials, Dr Ayako Miyazaki for critical reading of the manuscript, and Ms Rie Iwasaki for technical assistance. We also thank Dr Yoshikatsu Sato at WPI-ITbM Live Imaging Center for generous support in confocal microscopy.

Competing interests

The authors declare no competing or financial interests.

Funding

This work was supported by Minister of Education, Culture, Sports, Science and Technology/Japan Society for the Promotion of Science KAKENHI (JP26291057, JP16H01237 and JP17H06476 to K.U.T.; JP16H01462, JP17H03695 and JP17KT0017 to N.U.), and by the Toyoaki Foundation (to N.U.). K.U.T. is a Howard Hughes Medical Institute-Gordon and Betty Moore Foundation Investigator (GBMF3035). Confocal imaging was supported by the Japan Society for the Promotion of Science KAKENHI (JP16H06280 'Advanced Bioimaging Support') and by the Japan Advanced Plant Science Network. Deposited in PMC for release after 6 months.

Author contributions

Conceptualization: N.U.; Methodology: Y.K., N.U.; Validation: Y.K., N.U.; Formal analysis: Y.K., N.U.; Investigation: Y.K., N.U.; Data curation: Y.K., M.T., K.U.T., N.U.; Writing - original draft: Y.K., K.U.T., N.U.; Writing - review & editing: Y.K., K.U.T., N.U.; Visualization: Y.K., K.U.T., N.U.; Supervision: M.T., K.U.T., N.U.; Project administration: K.U.T., N.U.; Funding acquisition: K.U.T., N.U.

Supplementary information

Supplementary information available online at
http://dev.biologists.org/lookup/doi/10.1242/dev.156380.supplemental

References

Abrash, E. B., Davies, K. A. and Bergmann, D. C. (2011). Generation of signaling specificity in Arabidopsis by spatially restricted buffering of ligand-receptor interactions. *Plant Cell* **23**, 2864-2879.

Adibi, M., Yoshida, S., Weijers, D. and Fleck, C. (2016). Centering the organizing center in the arabidopsis thaliana shoot apical meristem by a combination of cytokinin signaling and self-organization. *PLoS ONE* **11**, e0147830.

Arata, Y., Nagasawa-Iida, A., Uneme, H., Nakajima, H., Kakimoto, T. and Sato, R. (2010). The phenylquinazoline compound S-4893 is a non-competitive cytokinin antagonist that targets Arabidopsis cytokinin receptor CRE1 and promotes root growth in Arabidopsis and rice. *Plant Cell Physiol.* **51**, 2047-2059.

Bemis, S. M., Lee, J. S., Shpak, E. D. and Torii, K. U. (2013). Regulation of floral patterning and organ identity by Arabidopsis ERECTA-family receptor kinase genes. *J. Exp. Bot.* **64**, 5323-5333.

Brand, U., Fletcher, J. C., Hobe, M., Meyerowitz, E. M. and Simon, R. (2000). Dependence of stem cell fate in Arabidopsis on a feedback loop regulated by CLV3 activity. *Science* **289**, 617-619.

Brand, U., Grunewald, M., Hobe, M. and Simon, R. (2002). Regulation of CLV3 expression by two homeobox genes in Arabidopsis. *Plant Physiol.* **129**, 565-575.

Busch, W., Miotk, A., Ariel, F. D., Zhao, Z., Forner, J., Daum, G., Suzaki, T., Schuster, C., Schultheiss, S. J., Leibfried, A. et al. (2010). Transcriptional control of a plant stem cell niche. *Dev. Cell* **18**, 849-861.

Chatfield, S. P., Capron, R., Severino, A., Penttila, P.-A., Alfred, S., Nahal, H. and Provart, N. J. (2013). Incipient stem cell niche conversion in tissue culture: using a systems approach to probe early events in WUSCHEL-dependent conversion of lateral root primordia into shoot meristems. *Plant J.* **73**, 798-813.

Chen, M.-K., Wilson, R. L., Palme, K., Ditengou, F. A. and Shpak, E. D. (2013). ERECTA family genes regulate auxin transport in the shoot apical meristem and forming leaf primordia. *Plant Physiol.* **162**, 1978-1991.

Chickarmane, V. S., Gordon, S. P., Tarr, P. T., Heisler, M. G. and Meyerowitz, E. M. (2012). Cytokinin signaling as a positional cue for patterning the apical-basal axis of the growing Arabidopsis shoot meristem. *Proc. Natl. Acad. Sci. USA* **109**, 4002-4007.

Fiers, M., Golemiec, E., Xu, J., van der Geest, L., Heidstra, R., Stiekema, W. and Liu, C. M. (2005). The 14-amino acid CLV3, CLE19, and CLE40 peptides trigger consumption of the root meristem in Arabidopsis through a CLAVATA2-dependent pathway. *Plant Cell* **17**, 2542-2553.

Godiard, L., Sauviac, L., Torii, K. U., Grenon, O., Mangin, B., Grimsley, N. H. and Marco, Y. (2003). ERECTA, an LRR receptor-like kinase protein controlling development pleiotropically affects resistance to bacterial wilt. *Plant J.* **36**, 353-365.

Gordon, S. P., Chickarmane, V. S., Ohno, C. and Meyerowitz, E. M. (2009). Multiple feedback loops through cytokinin signaling control stem cell number within the Arabidopsis shoot meristem. *Proc. Natl. Acad. Sci. USA* **106**, 16529-16534.

Gruel, J., Landrein, B., Tarr, P., Schuster, C., Refahi, Y., Sampathkumar, A., Hamant, O., Meyerowitz, E. M. and Jönsson, H. (2016). An epidermis-driven mechanism positions and scales stem cell niches in plants. *Sci. Adv.* **2**, e1500989.

Hirakawa, Y., Shinohara, H., Welke, K., Irle, S., Matsubayashi, Y., Torii, K. U. and Uchida, N. (2017). Cryptic bioactivity capacitated by synthetic hybrid plant peptides. *Nat. Commun.* **8**, 14318.

Horst, R. J., Fujita, H., Lee, J. S., Rychel, A. L., Garrick, J. M., Kawaguchi, M., Peterson, K. M. and Torii, K. U. (2015). Molecular framework of a regulatory circuit initiating two-dimensional spatial patterning of stomatal lineage. *PLoS Genet.* **11**, e1005374.

Huang, W., Pitorre, D., Poretska, O., Marizzi, C., Winter, N., Poppenberger, B. and Sieberer, T. (2015). ALTERED MERISTEM PROGRAM1 suppresses ectopic stem cell niche formation in the shoot apical meristem in a largely cytokinin-independent manner. *Plant Physiol.* **167**, 1471-1486.

Ikematsu, S., Tasaka, M., Torii, K. U. and Uchida, N. (2017). ERECTA-family receptor kinase genes redundantly prevent premature progression of secondary growth in the Arabidopsis hypocotyl. *New Phytol.* **213**, 1697-1709.

Kondo, T., Sawa, S., Kinoshita, A., Mizuno, S., Kakimoto, T., Fukuda, H. and Sakagami, Y. (2006). A plant peptide encoded by CLV3 identified by in situ MALDI-TOF MS analysis. *Science* **313**, 845-848.

Laux, T., Mayer, K. F., Berger, J. and Jurgens, G. (1996). The WUSCHEL gene is required for shoot and floral meristem integrity in Arabidopsis. *Development* **122**, 87-96.

Lee, C. and Clark, S. E. (2015). A WUSCHEL-independent stem cell specification pathway is repressed by PHB, PHV and CNA in arabidopsis. *PLoS ONE* **10**, e0126006.

Lee, J. S., Kuroha, T., Hnilova, M., Khatayevich, D., Kanaoka, M. M., McAbee, J. M., Sarikaya, M., Tamerler, C. and Torii, K. U. (2012). Direct interaction of ligand-receptor pairs specifying stomatal patterning. *Genes Dev.* **26**, 126-136.

Lee, J. S., Hnilova, M., Maes, M., Lin, Y.-C. L., Putarjunan, A., Han, S.-K., Avila, J. and Torii, K. U. (2015). Competitive binding of antagonistic peptides fine-tunes stomatal patterning. *Nature* **522**, 439-443.

Leibfried, A., To, J. P. C., Busch, W., Stehling, S., Kehle, A., Demar, M., Kieber, J. J. and Lohmann, J. U. (2005). WUSCHEL controls meristem function by direct regulation of cytokinin-inducible response regulators. *Nature* **438**, 1172-1175.

Long, J. A., Moan, E. I., Medford, J. I. and Barton, M. K. (1996). A member of the KNOTTED class of homeodomain proteins encoded by the STM gene of Arabidopsis. *Nature* **379**, 66-69.

Mähönen, A. P., Bonke, M., Kauppinen, L., Riikonen, M., Benfey, P. N. and Helariutta, Y. (2000). A novel two-component hybrid molecule regulates vascular morphogenesis of the Arabidopsis root. *Genes Dev.* **14**, 2938-2943.

Mandel, T., Moreau, F., Kutsher, Y., Fletcher, J. C., Carles, C. C. and Eshed Williams, L. (2014). The ERECTA receptor kinase regulates Arabidopsis shoot apical meristem size, phyllotaxy and floral meristem identity. *Development* **141**, 830-841.

Mandel, T., Candela, H., Landau, U., Asis, L., Zelinger, E., Carles, C. C. and Williams, L. E. (2016). Differential regulation of meristem size, morphology and organization by the ERECTA, CLAVATA and class III HD-ZIP pathways. *Development* **143**, 1612-1622.

Mayer, K. F. X., Schoof, H., Haecker, A., Lenhard, M., Jürgens, G. and Laux, T. (1998). Role of WUSCHEL in regulating stem cell fate in the Arabidopsis shoot meristem. *Cell* **95**, 805-815.

Meng, W., Cheng, Z. J., Sang, Y. L., Zhang, M. M., Rong, X. F., Wang, Z. W., Tang, Y. Y. and Zhang, X. S. (2017). Type-B ARABIDOPSIS RESPONSE REGULATORs is critical to the specification of shoot stem cell niche by dual regulation of WUSCHEL. *Plant Cell* **29**, 1357-1372.

Meyerowitz, E. M. (1997). Genetic control of cell division patterns in developing plants. *Cell* **88**, 299-308.

Miwa, H., Kinoshita, A., Fukuda, H. and Sawa, S. (2009). Plant meristems: CLAVATA3/ESR-related signaling in the shoot apical meristem and the root apical meristem. *J. Plant Res.* **122**, 31-39.

Ogawa, M., Shinohara, H., Sakagami, Y. and Matsubayashi, Y. (2008). Arabidopsis CLV3 peptide directly binds CLV1 ectodomain. *Science* **319**, 294.

Schoof, H., Lenhard, M., Haecker, A., Mayer, K. F., Jürgens, G. and Laux, T. (2000). The stem cell population of Arabidopsis shoot meristems in maintained by a regulatory loop between the CLAVATA and WUSCHEL genes. *Cell* **100**, 635-644.

Sessions, A., Weigel, D. and Yanofsky, M. F. (1999). The Arabidopsis thaliana MERISTEM LAYER 1 promoter specifies epidermal expression in meristems and young primordia. *Plant J.* **20**, 259-263.

Shpak, E. D., Berthiaume, C. T., Hill, E. J. and Torii, K. U. (2004). Synergistic interaction of three ERECTA-family receptor-like kinases controls Arabidopsis organ growth and flower development by promoting cell proliferation. *Development* **131**, 1491-1501.

Sonoda, Y., Yao, S.-G., Sako, K., Sato, T., Kato, W., Ohto, M.-A., Ichikawa, T., Matsui, M., Yamaguchi, J. and Ikeda, A. (2007). SHA1, a novel RING finger protein, functions in shoot apical meristem maintenance in Arabidopsis. *Plant J.* **50**, 586-596.

Tameshige, T., Okamoto, S., Lee, J. S., Aida, M., Tasaka, M., Torii, K. U. and Uchida, N. (2016). A secreted peptide and its receptors shape the auxin response pattern and leaf margin morphogenesis. *Curr. Biol.* **26**, 2478-2485.

Uchida, N., Igari, K., Bogenschutz, N. L., Torii, K. U. and Tasaka, M. (2011). Arabidopsis ERECTA-family receptor kinases mediate morphological alterations stimulated by activation of NB-LRR-Type UNI Proteins. *Plant Cell Physiol.* **52**, 804-814.

Uchida, N., Lee, J. S., Horst, R. J., Lai, H.-H., Kajita, R., Kakimoto, T., Tasaka, M. and Torii, K. U. (2012). Regulation of inflorescence architecture by intertissue layer ligand-receptor communication between endodermis and phloem. *Proc. Natl. Acad. Sci. USA* **109**, 6337-6342.

Uchida, N., Shimada, M. and Tasaka, M. (2013). ERECTA-family receptor kinases regulate stem cell homeostasis via buffering its cytokinin responsiveness in the shoot apical meristem. *Plant Cell Physiol.* **54**, 343-351.

Wang, J., Tian, C., Zhang, C., Shi, B., Cao, X., Zhang, T. Q., Zhao, Z., Wang, J. W. and Jiao, Y. (2017). Cytokinin signaling activates WUSCHEL expression during axillary meristem initiation. *Plant Cell* **29**, 1373-1387.

Werner, T., Motyka, V., Laucou, V., Smets, R., Van Onckelen, H. and Schmulling, T. (2003). Cytokinin-deficient transgenic Arabidopsis plants show multiple developmental alterations indicating opposite functions of cytokinins in the regulation of shoot and root meristem activity. *Plant Cell* **15**, 2532-2550.

Yadav, R. K., Girke, T., Pasala, S., Xie, M. and Reddy, G. V. (2009). Gene expression map of the Arabidopsis shoot apical meristem stem cell niche. *Proc. Natl. Acad. Sci. USA* **106**, 4941-4946.

Yadav, R. K., Tavakkoli, M. and Reddy, G. V. (2010). WUSCHEL mediates stem cell homeostasis by regulating stem cell number and patterns of cell division and differentiation of stem cell progenitors. *Development* **137**, 3581-3589.

Yadav, R. K., Tavakkoli, M., Xie, M., Girke, T. and Reddy, G. V. (2014). A high-resolution gene expression map of the Arabidopsis shoot meristem stem cell niche. *Development* **141**, 2735-2744.

Zurcher, E., Tavor-Deslex, D., Lituiev, D., Enkerli, K., Tarr, P. T. and Muller, B. (2013). A robust and sensitive synthetic sensor to monitor the transcriptional output of the cytokinin signaling network in planta. *Plant Physiol.* **161**, 1066-1075.

Table S1. Number of floral organs. The average value ± S.D. is shown.

	Pistil	Stamen	Sepal	Petal	n
Wild type	1±0	5.6±0.52	4±0	4±0	10
er erl1 erl2	1±0	4.3±1.49	4.1±0.73	2.4±1.17	10
wus	0±0	0.81±0.6	3.18±0.75	2.45±0.82	11
wus er erl1 erl2	1±0	3.92±0.51	3.25±0.87	1.75±0.62	12

Table S2. Primer sets used in this study

CLV3 (qRT-PCR)	TCTTCTGCTTCTTGTTCCTTCA TCATGTAGTCCTAAACCCTTCGT
STM (qRT-PCR)	CAAATGGCCTTACCCTTCG GCCGTTTCCTCTGGTTTATG
ARR1 (qRT-PCR)	GCGCACTTCTTAAGCAGGAA TGGAGTATGCGTCAAAGTCG
ARR2 (qRT-PCR)	CGTTGATGATGATCCAACTTGT TCCGAAGCAGAGACAATGC
ARR10 (qRT-PCR)	CTTCAGCGCTGCCAATATC GTTCTCCCTCAACAACTCCAA
ARR11 (qRT-PCR)	GGTCTTGAATTAGACCTCCCTGT TGTTGCACTCCCTTCATCAC
ARR12 (qRT-PCR)	CTCCACGATGAAGCAGGAA AACTAAACCCTCCATATCCCAAA
ARR14 (qRT-PCR)	TGTTTCTGTGGCGGTTCAT TGTTAACGTCACCTCTCTGTCTG
AHK2 (qRT-PCR)	CCCATATTGTATCGGTCGACAT TTGCCCGTAAGATGTTTTCA
AHK3 (qRT-PCR)	AGATGCCAGAAATGGATGGA ATCAAAGCCTCCCCATTCTT
AHK4 (qRT-PCR)	GGCACTCAACAATCATCAAG TCTTTCTCGGCTTTTCTGAC
WUS (promoter)	CAACGTCGACCACTCCTATGTTATTAGCTAAAATGTTTAG CAACGTCGACGTGTGTTTGATTCGACTTTTGTTC
EPFL1 (promoter)	CCCCCAAGCTTACCGAGATTTAAGTCATGGTTATATAC TCCCCCGGGGTTTTGAGTTGGATTCAAGAATTACTAC

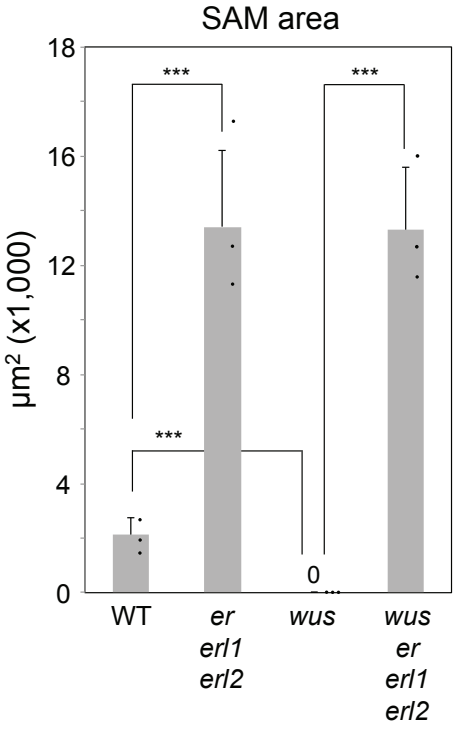

Figure S1. SAM loss in *wus* is recovered in *er erl1 erl2*.
SAM area in 10-day-old plants calculated from scanning electron microscopy images using ImageJ. The mean of three independent samples ± SD is shown for each genotype. ***P<0.005, Student's t-test (two-tailed).

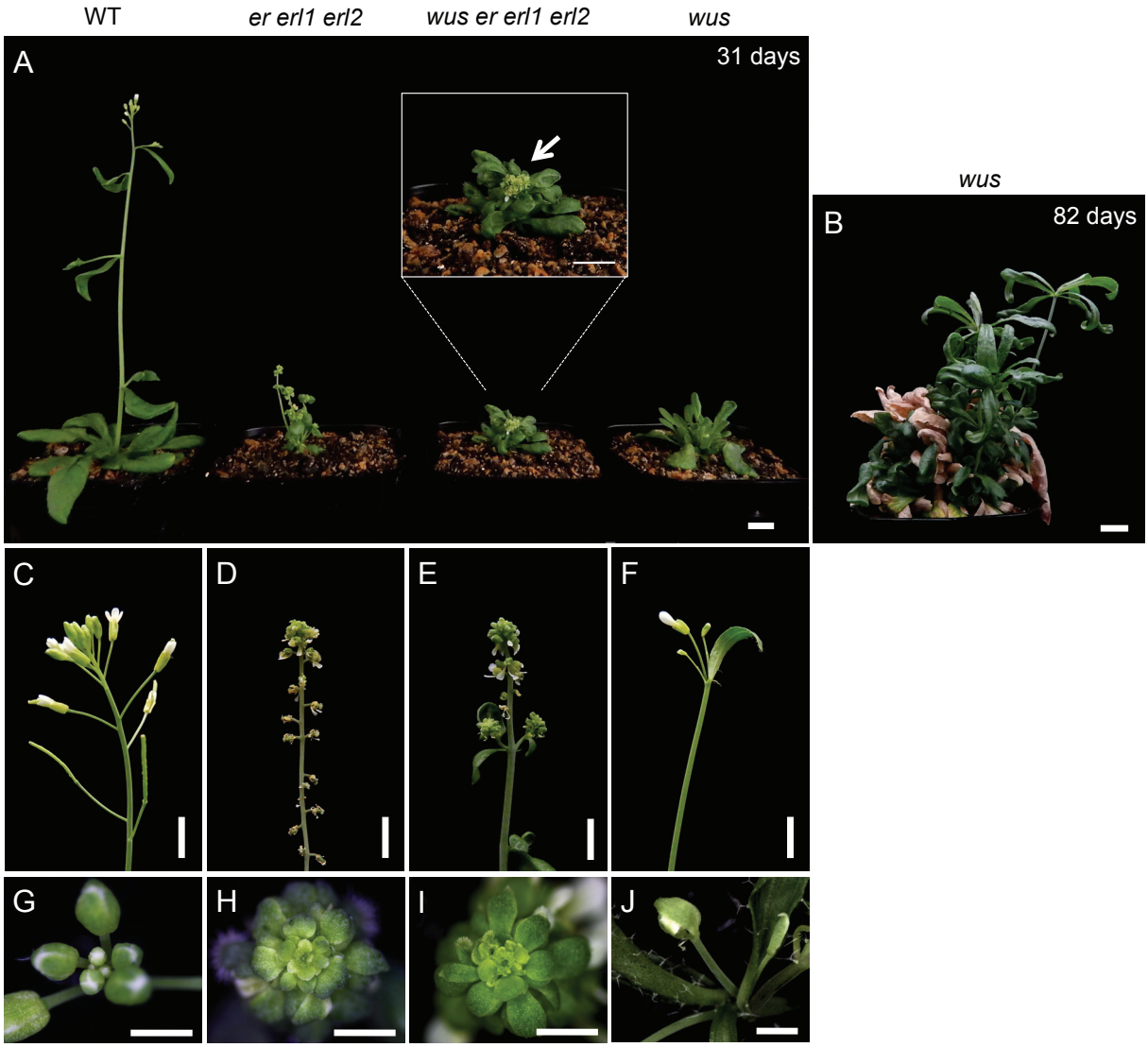

Figure S2. Altered inflorescence morphology in *wus* is rescued by *er erl1 erl2*.
(A, B) Plant morphology of various genotypes at 31 (A) and 82 (B) days after germination. The arrow indicates the emergence of the inflorescence stem in *wus er erl1 erl2*. Inflorescence stem emergence is severely delayed in *wus* mutants. Bars=10 mm. **(C–F)** Photos of the inflorescence structure of various genotypes. Bars=5 mm. **(G–J)** Photos of the inflorescences of various genotypes. Bars=1 mm.

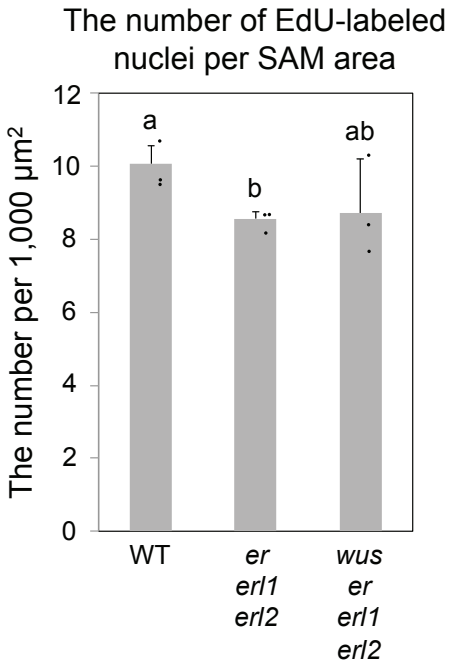

Figure S3. The number of EdU-labeled nuclei normalized to the SAM area.
The number of EdU-labeled nuclei in the SAM were normalized to the area of small cells characteristic of the SAM. Note that, because the SAM is lost in the *wus* mutant (Figs. 1–3), the number of EdU positive cells could not be divided by the SAM area for the *wus* mutant. Therefore this graph does not include the value of the *wus* mutant. No significant difference was detected by Tukey's HSD test ($P<0.05$) among data sharing the same alphabet.

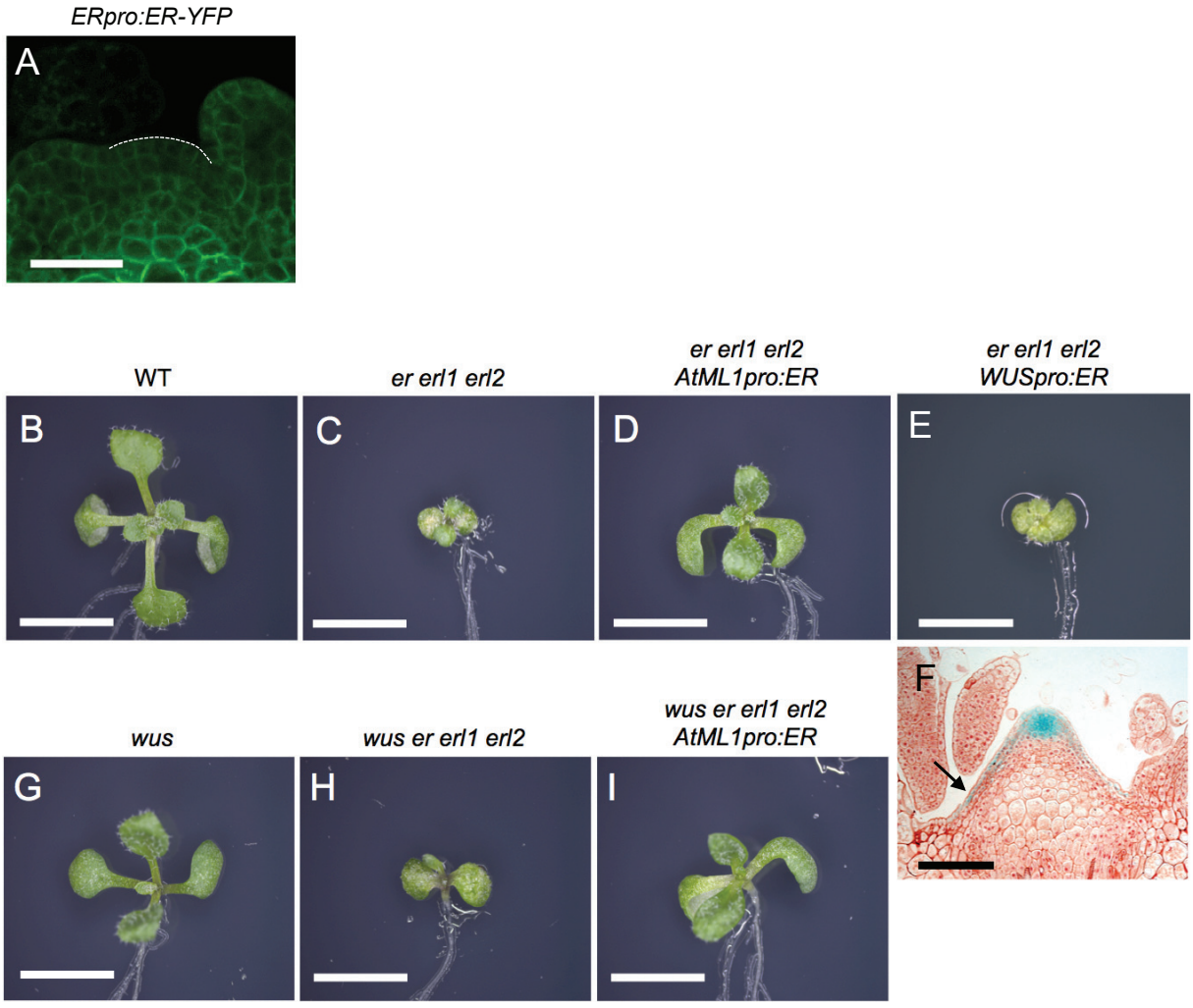

Figure S4. *AtML1pro:ER* largely rescues seedling defects of *er*-family mutants.
(A) *ERpro:ER-YFP* signals in the 8-day-old SAM in *er* mutant background. Note that no YFP signal was detected in wild type without the transgene under the same microscope setting (data not shown). Bars=100 μm. **(B–E, G–I)** 10-day-old seedlings of various genotypes. Bars=5 mm. **(F)** *CLV3pro:GUS* signals in a section of the 8-day-old *er erl1 erl2 WUSpro:ER* SAM. The arrow indicates *CLV3pro:GUS* signal localized to the epidermis. Bar=100 μm.

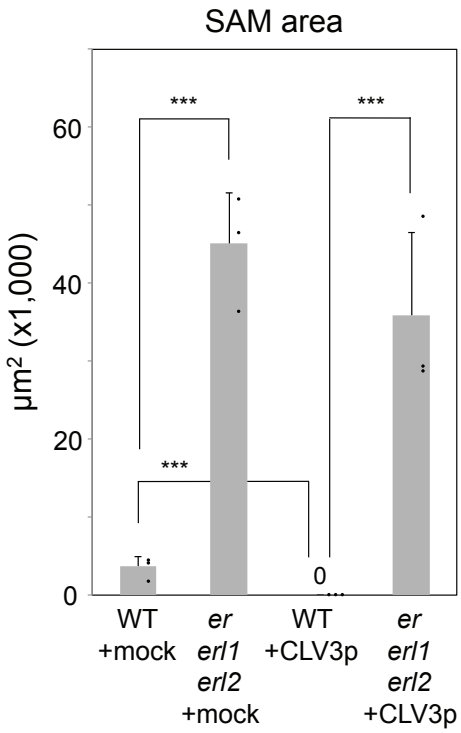

Figure S5. Effect of CLV3 peptide treatment on SAM area.
The SAM areas of 12-day-old plants were quantified via ImageJ analysis of scanning electron microscopy images. The mean of three independent samples for each genotype ± SD is shown. ***P<0.005, Student's t-test (two-tailed).

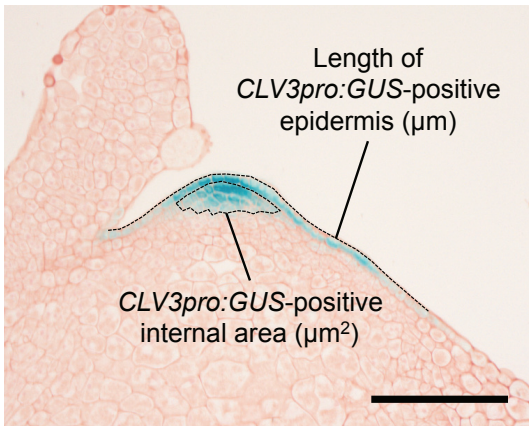

Figure S6. Explanation of the method employed to measure both the length of the SAM epidermis (µm) and the SAM internal area (µm^2) expressing *CLV3pro:GUS*.
Sections from plants expressing *CLV3pro:GUS* were analyzed using ImageJ. An annotated image from Fig. 5T is shown as an example.

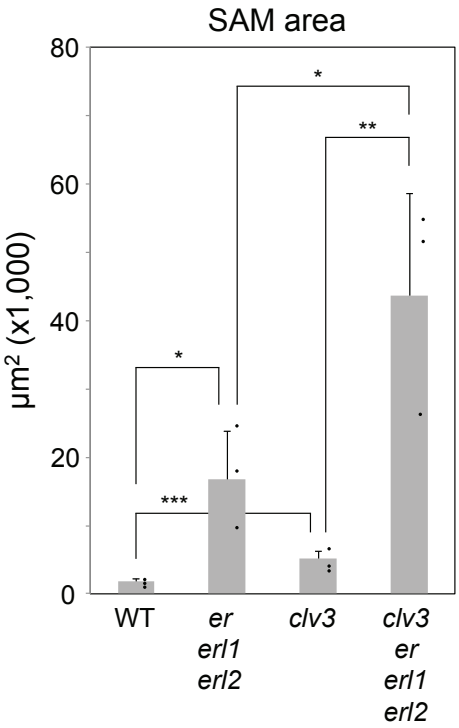

Figure S7. The SAM in *clv3 er erl1 erl2* is larger than that in *clv3* and *er erl1 erl2*.
SAM areas of 10-day-old plants were quantified via ImageJ analysis of scanning electron microscopy images. The mean of three independent samples for each genotype ± SD is shown. **P*<0.05, ***P*<0.01, ****P*<0.005, Student's *t*-test (two-tailed).

Figure S8. Effect of CLV3 peptide treatment on root growth.
Root growth in 10-day-old seedlings of wild type (WT) and *er erl1 erl2* was observed following 5 μM CLV3 peptide treatment (CLV3p). Bars=1 cm.

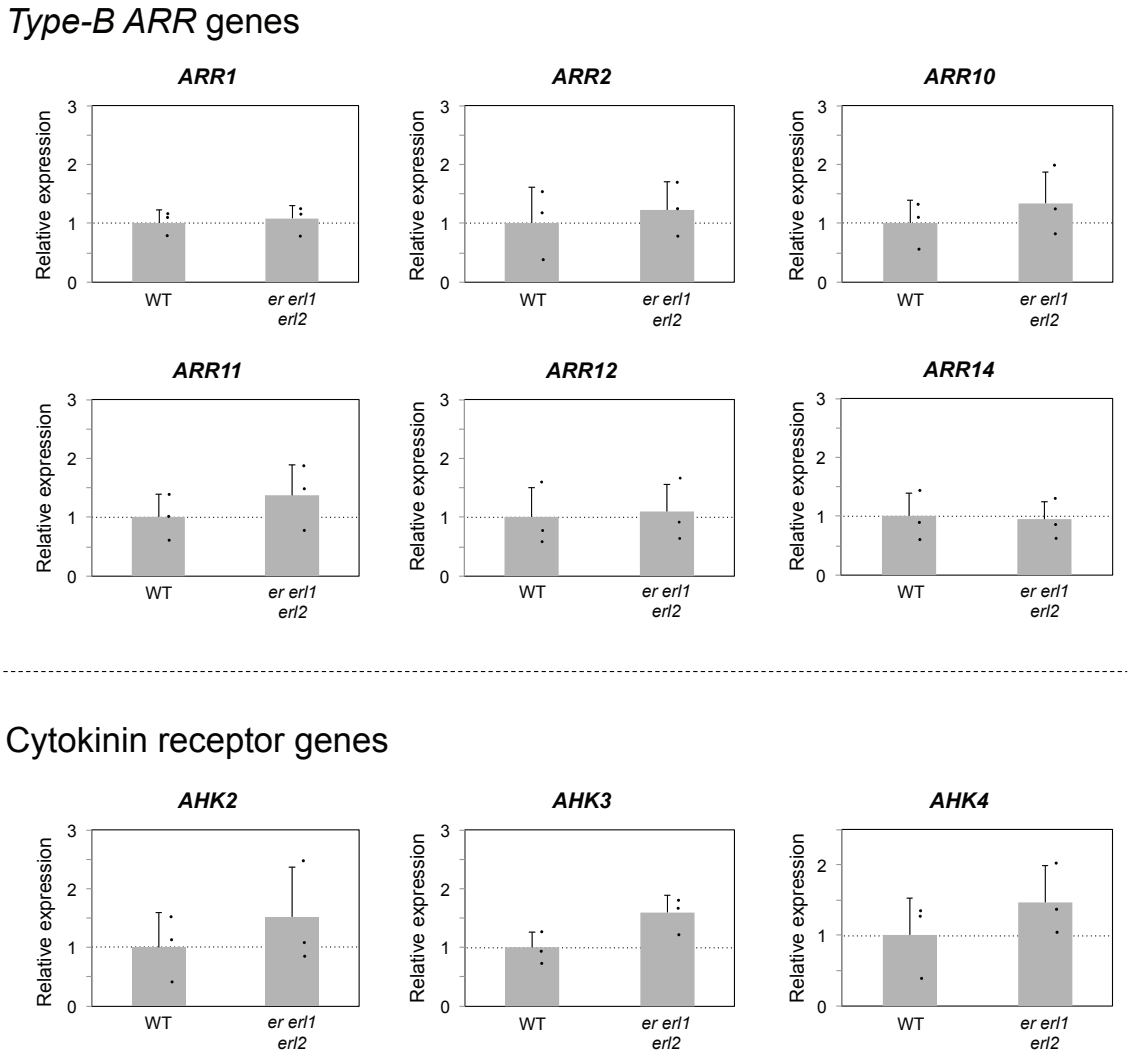

Figure S9. Expression levels of *Type-B ARR* and cytokinin receptor genes.
Gene expression levels in shoot apices as normalized against *β-TUBULIN* expression. Expression levels are related to that in the wild type, which was set to 1. Twenty individual plants were pooled for each sample. The mean of three biological replicates ± SD is shown.

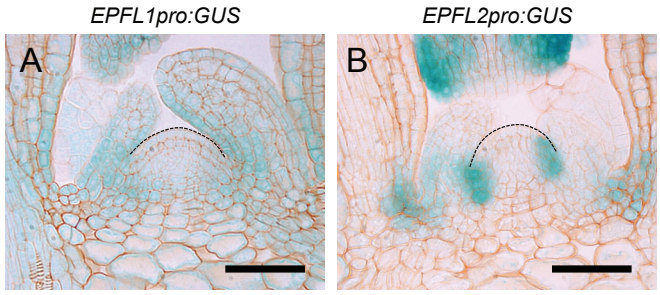

Figure S10. Expression patterns of *EPFL1pro:GUS* and *EPFL2pro:GUS* in the SAM.
Signals of *EPFL1pro:GUS* (A) and *EPFL2pro:GUS* (B) in sections of SAM tissue from 10-day-old wild-type plants. Dotted lines outline SAM regions. Bars=50 μm. Note that GUS signals from *EPFL2pro:GUS* are detected at boundary tissues between the SAM and leaf primordia.